Inorganic Chemistry

Article

pubs.acs.org/IC

^{17}O NMR and Density Functional Theory Study of the Dynamics of the Carboxylate Groups in DOTA Complexes of Lanthanides in Aqueous Solution

Florian Mayer,[†] Carlos Platas-Iglesias,[‡] Lothar Helm,[§] Joop A. Peters,[†] and Kristina Djanashvili*,[†]

[†]Biocatalysis and Organic Chemistry, Department of Biotechnology, Delft University of Technology, Julianalaan 136, 2628 BL Delft, The Netherlands

[‡]Departamento de Química Fundamental, Campus da Zapateira, Universidade da Coruña, Rúa da Fraga 10, 15008 A Coruña, Spain

[§]Laboratoire de Chimie Inorganique et Bioinorganique, Ecole Polytechnique Fédérale de Lausanne, CH-1015, Switzerland

Supporting Information

ABSTRACT: The rotation of the carboxylate groups in DOTA (DOTA = 1,4,7,10-tetraazacyclododecane-1,4,7,10-tetraacetate) complexes of several lanthanide ions and Sc^{3+} was investigated with density functional theory (DFT) calculations and with variable temperature ^{17}O NMR studies at 4.7−18.8 T. The data obtained show that the rotation is much slower than the other dynamic processes taking place in these complexes. The exchange between the bound and unbound carboxylate oxygen atoms for the largest Ln^{3+} ions (La^{3+}→Sm^{3+}) follows a pathway via a transition state in which both oxygens of the carboxylate group are bound to the Ln^{3+} ion, whereas for the smaller metal ions (Tm^{3+}, Lu^{3+}, Sc^{3+}) the transition state has a fully decoordinated carboxylate group. The activation free energies show a steady increase from about 75 to 125−135 kJ·mol^{-1} going from La^{3+} to Lu^{3+}. This computed trend is consistent with the results of the ^{17}O NMR measurements. Fast exchange between bound and unbound carboxylate oxygen atoms was observed for the diamagnetic La-DOTA, whereas for Pr-, Sm-, Lu-, and Sc-DOTA the exchange was slow on the NMR time scale. The trends in the linewidths for the various metal ions as a function of the temperature agree with trends in the rates as predicted by the DFT calculations.

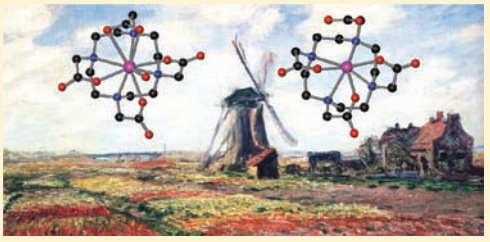

INTRODUCTION

The macrocyclic compound DOTA (DOTA = 1,4,7,10-tetraazacyclododecane-1,4,7,10-tetraacetate) forms complexes with lanthanide ions with high thermodynamic stability and kinetic inertness with respect to the release of the metal ion.[1,2] Consequently, these complexes have found widespread use in diagnostic and therapeutic medicine. Notably, [Gd(DOTA)-(H_2O)]$^-$ is being successfully applied as a contrast agent in magnetic resonance imaging (MRI).[3−5] The contrast enhancement is achieved by the increase of the longitudinal relaxation rate of water protons in the vicinity of the paramagnetic complex. The efficiency of a contrast agent is usually expressed by its relaxivity (the relaxation rate enhancement in s^{-1} per mM concentration of Gd^{3+}), which is determined by several parameters including the electronic relaxation rate of Gd^{3+}, the rotational dynamics of the complex, and the exchange rate of the Gd^{3+} coordinated water molecule.

Currently, a great deal of research is devoted to molecular imaging applications of MRI.[6,7] In this case, the low intrinsic sensitivity of this technique is often a limitation, and therefore, relatively large local concentrations of a contrast agent are required to obtain an observable contrast enhancement. This may be achieved by employing targeted agents that can deliver multiple Gd^{3+}-chelates to the sites of interest. Obviously, it is important that each of these Gd^{3+} chelates has optimal relaxivity. For the rational design of MRI contrast agents with optimal relaxivity, detailed understanding of the structural parameters controlling the relaxivity is indispensable.

The DOTA ligand is known to bind Ln^{3+} ions octadentately through its 4 N atoms and an O-atom of each of the 4 carboxylate functions.[8−11] The ethylene groups of the macrocycle adopt two different gauche orientations (λ or δ), whereas the pendant acetate arms are twisted around the Ln^{3+} ion in two orientations, Δ and Λ. In solution two diastereomeric forms, $\Delta(\delta\delta\delta\delta)/\Lambda(\lambda\lambda\lambda\lambda)$ and $\Delta(\lambda\lambda\lambda\lambda)/\Lambda(\delta\delta\delta\delta)$, occur, which differ in the mutual orientation of the parallel planes formed by the Ln-bound N- and O-atoms (see Scheme 1). The twist angles between these planes are about +40 and −24° corresponding to square antiprismatic (SAP, often labeled M) and twisted square antiprismatic (TSAP, often labeled m) coordination geometries, respectively. The ratio of SAP/TSAP changes along the lanthanide series: La-DOTA occurs predominantly in the TSAP form, whereas for Yb-DOTA the SAP form predominates. A hydration equilibrium is superimposed on this conformational equilibrium to give sets of both 8- and 9-coordinated species. The 9-coordinate species predominate for Ln = La to Er, whereas the 8-coordinate

Received: June 29, 2011
Published: November 30, 2011

Scheme 1. Schematic Representation of the Conformational Isomers of Ln-DOTA Complexes[a]

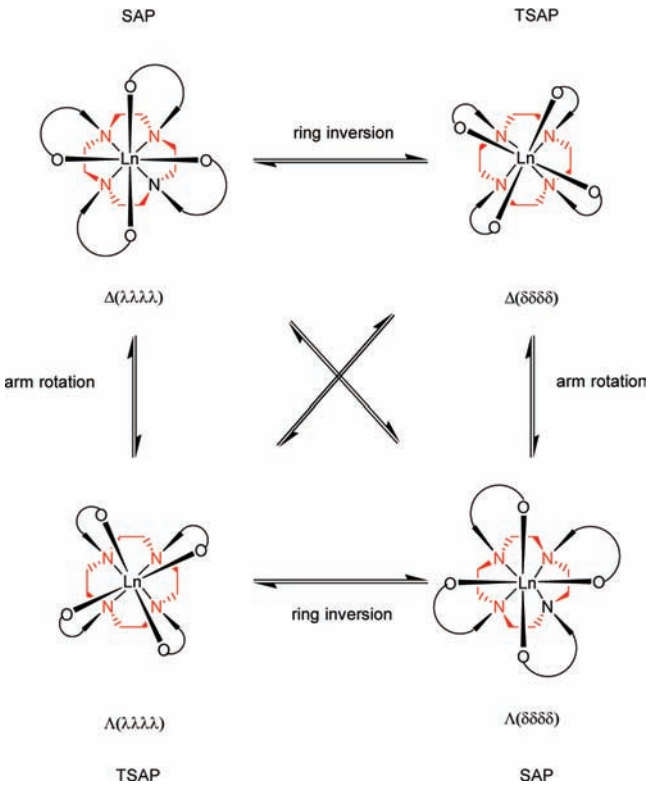

[a]Two sets occur: 8-coordinated and 9-coordinated; in the latter, a water molecule caps the O_4 plane. The SAP forms have not been observed for the 8-coordinated complexes.

Ln-complexes have only been observed for the heavier lanthanides (Er→Lu) and then exclusively in the TSAP geometry.[11] Both the SAP and TSAP isomers of $[Sc(DOTA)]^-$ are known to exist in solution as 8-coordinate species.

With the use of variable temperature ^{13}C NMR on $[Nd(DOTA)]^-$ and ^1H EXSY on $[Yb(DOTA)]^-$, it has been shown that the four isomers of the 9-coordinated species all interconvert. On the basis of extensive variable temperature and pressure NMR studies, a semiquantitative energy diagram for the various rearrangements in Ln-DOTA complexes has been proposed.[11]

The exchange rate of water molecules between the Ln-DOTA complexes and the bulk has been shown to be significantly higher for the TSAP than for the SAP form.[12−16] For $[Gd(DOTA)(H_2O)]^-$, the overall water exchange rate is 4.1×10^6 s^{-1},[17] whereas the interconversion rates of the various forms of the DOTA ligand are several orders of magnitude lower.[10,11]

A question that remains to be answered is whether the carboxylate groups are immobilized or rotating in the Ln-DOTA complexes. Therefore, we here evaluate the rates of interconversion of the carboxylate oxygen atoms in Ln-DOTA complexes, using ^{17}O NMR and density functional theory (DFT) calculations. Previously, Purgel et al. have reported DFT calculations on SAP and TSAP isomers of $[Eu(DOTA)(H_2O)]^-$ and $[Lu(DOTA)]^-$.[18] To get some insight into the effect of the decrease of the ionic radius on the carboxylate rotation we first performed similar calculations on various isomers of DOTA complexes with selected Ln^{3+} ions along the lanthanide series from La^{3+} to Lu^{3+}. For comparison Sc, a rare earth metal with a significantly smaller ionic radius than the lanthanides was included in this study. Next, these optimal structures were used to model the transition state of the carboxylate rotation. The rotation rates obtained are compared with the results of a variable temperature ^{17}O NMR study on Ln-DOTA complexes with ^{17}O-enriched carboxylate functions. Finally, the results are discussed in view of the known rates of hydration and isomerization of Ln-DOTA complexes.

EXPERIMENTAL SECTION

Materials. H_4DOTA was obtained from Chematech, 21000 Dijon, France; $CoCl_2$, $ScCl_3$, and $LnCl_3$ (as hydrates) were purchased from Sigma-Aldrich, St. Louis, MO 63103, U.S.A. These chemicals were used as obtained. Water was purified with a Milli-Q system.

Synthesis of ^{17}O Enriched H_4DOTA and Preparation of Metal Complexes Thereof. H_4DOTA (1 g, 2.47 mmol) was stirred in 4 mL of water. After 10 min 1 mL of ^{17}O enriched water (10% ^{17}O) and 1 drop of concentrated HCl (36%) were added. The resulting slurry was heated at 90 °C for 18 h under stirring and then cooled to room temperature. Finally, the product was freeze-dried to obtain the ^{17}O enriched H_4DOTA as a white powder (920 mg, 2.28 mmol, 92%). The degree of enrichment was determined by ESI-MS. The ^1H and ^{13}C NMR spectra were identical to those of the starting material.

The metal complexes were prepared by mixing solutions of the ^{17}O enriched H_4DOTA (120 mg, 0.29 mmol) in 3 mL of water and the appropriate metal chloride (0.26 mmol, 95 mol %) in 0.5 mL of water. The pH was maintained at 5 by adding NaOH (0.1 M) with a Metrohm Dosimeter 665. After the consumption of NaOH had stopped the solution was stirred for another 3 h and then freeze-dried to result in the product as a powder. ^1H and ^{13}C NMR spectra of the complexes were identical with those of authentic samples of the known compounds, apart from the resonances of the small excess of free ligand (5%). The amount of Ln-DOTA complexes in the various samples was determined by quantitative ^1H NMR measured in the presence of weighed amounts of *tert*-butanol.

A typical sample for NMR measurements was prepared by dissolving 0.12 mmol of the concerning metal-DOTA complex in 0.5 mL of D_2O. The pH was adjusted to 6.3 by adding either a DCl or a NaOD solution in D_2O, followed by a filtration over a hydrophilic Nylon syringe filter (0.2 μm). For the measurements in 10 mm sapphire tubes, larger samples were prepared by dissolving 0.6 mmol of the compounds in 2 mL of D_2O, adjusting the pH, and filtering in the same way.

Measurements with $CoCl_2$ were done at 300 MHz in 5 mm NMR tubes. The samples were prepared by adding portions of an aqueous $CoCl_2$ solution (0.12 mmol in 0.1 mL) to $Ln(DOTA)^-$ or $Sc(DOTA)^-$ samples.

Physical Methods. NMR spectra were measured on a Bruker Avance 200, Varian Inova-Unity 300, Bruker Avance 400 or a Bruker Avance 800 spectrometer. On Avance 200 and 800 spectrometers, spectra were measured in the temperature range of 25−147 °C using closed 10 mm sapphire sample tubes under pressurized argon (~10 bar).[19] Peak positions in the ^{17}O NMR spectra were measured with respect to the resonance of the solvent (D_2O). Linewidths and integrals of NMR signals were obtained by fitting Lorentzian functions to the experimental spectra using the NMRICMA program[20] for MATLAB. The adjustable parameters are the resonance frequency, intensity, line width, baseline, and phasing.

All other fittings of the experimental data were performed using the computer program Micromath Scientist version 2.0 (Salt Lake City, UT).

Computational Details. All calculations were performed using hybrid DFT with the restricted B3LYP exchange-correlation functional,[21,22] and the Gaussian 09 package (Revision A.02).[23] On the grounds of previous investigations on related Ln^{3+} complexes,[18,24] full geometry optimizations of the $[Ln(DOTA)(H_2O)]^-$ (Ln = La, Nd, Sm, Tb, or Ho) and $[Ln(DOTA)]^-$ (Ln = Tm or Lu) systems were performed in the gas phase by using the effective core potential (ECP)

dx.doi.org/10.1021/ic201393n | *Inorg. Chem.* 2012, 51, 170−178

Table 1. Geometrical Parameters of Experimental (X-ray) and Calculated Structures for the Two Isomers of $[Nd(DOTA)(H_2O)]^-$, $[Tm(DOTA)]^-$, and $[Sc(DOTA)]^-$ Complexes[a]

	$[Nd(DOTA)(H_2O)]^-$			$[Tm(DOTA)]^-$			$[Sc(DOTA)]^-$		
	SAP	SAP	TSAP[b]	SAP[b]	TSAP	TSAP	SAP	SAP	TSAP[b]
	calc	exp	calc	calc	calc	exp	calc	exp	calc
Ln−N	2.833	2.704	2.864	2.700	2.733	2.529	2.637	2.446	2.685
Ln−O	2.433	2.416	2.436	2.268	2.267	2.280	2.101	2.154	2.098
$Ln-O_W$	2.631	2.508	2.622						
ω[c]	37.6	37.8	−24.9	39.4	−26.3	−24.4	41.2	41.2	−28.2
$Ln-P_O$[d]	0.587	0.684	0.643	0.748	0.796	1.064	0.765	1.007	0.785
$Ln-P_N$[e]	1.837	1.676	1.907	1.666	1.740	1.466	1.596	1.327	1.689
P_O-P_N[f]	2.424	2.360	2.551	2.414	2.631	2.530	2.360	2.334	2.474

[a]Distances (Å); the average values of bond distances to the oxygen atoms of the P_O (Ln−O) and P_N (Ln−N) planes are reported; O_W, oxygen atom of the inner-sphere water molecule. [b]No experimental data available. [c]Mean twist angle (deg) of the upper and lower planes. [d]Distance between the lanthanide and the least-squares plane defined by the coordinated oxygen atoms, P_O. [e]Distance between the lanthanide and the least-squares plane defined by the nitrogen atoms, P_N. [f]Distance between the centroids of the P_O and P_N planes.

of Dolg et al. and the related [5s4p3d]-GTO valence basis set for the lanthanides,[25] and the 6-31G(d) basis set for C, H, N, and O atoms. This ECP includes 46 + $4f^n$ electrons in the core, leaving the outermost 11 electrons to be treated explicitly. The use of large core ECPs has been justified by the fact that 4f orbitals do not significantly contribute to bonding because of their limited radial extension as compared to the 5d and 6s shells.[26,27] In the case of the $[Sc(DOTA)]^-$ system, the standard 6-31G(d) basis set was used for all atoms (including Sc). No symmetry constraints have been imposed during the optimizations. The default values for the integration grid ("fine") and the self-consistent field (SCF) energy convergence criteria (10^{-6}) were used. The stationary points found on the potential energy surfaces as a result of the geometry optimizations have been tested via frequency analysis to represent energy minima rather than saddle points. The relative free energies of the SAP and TSAP conformations were calculated at the same computational level, and they include nonpotential-energy contributions (zero point energies and thermal terms) obtained through frequency analysis.

The exchange between coordinated and noncoordinated oxygen atoms of acetate groups of DOTA was investigated by means of the synchronous transit-guided quasi-Newton method.[28] The nature of the saddle points was characterized by frequency analysis. The free energy barriers include nonpotential energy contributions obtained from frequency calculations. To evaluate the bulk solvent effects on the activation barriers, single point energy calculations were performed in aqueous solution at all critical points on the geometries optimized in the gas phase. Solvent effects were evaluated by using the polarizable continuum model (PCM), in which the solute cavity is built as an envelope of spheres centered on atoms or atomic groups with appropriate radii. In particular, we used the integral equation formalism (IEFPCM) variant as implemented in Gaussian 09.[29]

RESULTS AND DISCUSSION

Computation of Molecular Geometries and Conformational Energies. Aiming to obtain a deeper understanding of the conformational properties of the Ln^{3+} and Sc^{3+} complexes of DOTA we have performed full geometry optimizations of the $[Ln(DOTA)(H_2O)]^-$ (Ln = La, Nd, Sm, Tb or Ho), $[Ln(DOTA)]^-$ (Ln = Tm or Lu) and $[Sc(DOTA)]^-$ systems at the B3LYP level. As expected, these calculations provide the SAP and TSAP isomers as minimum energy conformations. The main geometrical parameters calculated for the Nd^{3+}, Tm^{3+}, and Sc^{3+} complexes (see Supporting Information, Table S1) are compared to the experimental data obtained from X-ray diffraction in Table 1.[30] The distances between the metal ions and the donor atoms of the ligand decrease along the lanthanide series, as usually observed for Ln^{3+} complexes as a consequence of the lanthanide contraction.[31] The average Ln−O distances obtained from DFT calculations are in excellent agreement with the experimental values. The coordination polyhedron around the lanthanide ion may be considered to be composed of two virtually parallel pseudo planes: the four amine nitrogen atoms define the lower plane (P_N), while the four oxygen atoms coordinated to the metal ion define the upper plane (P_O). The mean twist angles of these parallel planes (ω) are also in very good agreement with the experimental values. As observed previously for related systems,[18] the main discrepancy between the experimental and calculated geometries arises from the Ln−N distances. Indeed, the optimized geometries present substantially longer Ln−N bond distances than the solid state structures, which is also reflected in the $Ln-P_N$ and $Ln-P_O$ values. This can be partially ascribed, in the case of Ln^{3+} complexes, to the fact that the large-core ECPs usually provide bond distances that are 0.02−0.07 Å longer than the experimental ones.[32]

To test the effect of the solvent on the geometries of these complexes we have performed geometry optimizations of $[La(DOTA)(H_2O)]^-$ and $[Lu(DOTA)]^-$ in aqueous solution by using a polarizable continuum model (PCM). Our results show that the inclusion of solvent effects results in a relatively important shortening of the Ln−N bond distances (about 0.03−0.07 Å), while the Ln−O bonds are only slightly increased (<0.04 Å). However, it is well-known that geometry optimizations in solution based on the PCM model suffer from convergence problems such as slow convergence, no convergence, or convergence to higher energetic conformations.[33,34] The main goal of this work is to study the exchange between coordinated and noncoordinated oxygen atoms of acetate groups in Ln^{3+}-DOTA complexes, which requires the characterization of energy minima and transition states by using frequency analysis. Geometry optimizations of the transition states involved in this exchange process suffered from convergence difficulties. Thus, in the following we will focus on the geometries of the different complexes optimized in the gas phase, even when they are expected to possess considerably long Ln−N distances in comparison to experimental data.

The relative populations of the TSAP and SAP conformations of Ln^{3+} and Sc^{3+} complexes of DOTA have been studied in detail by using NMR spectroscopy.[11] One can easily derive relative free energies from the populations of the two isomers using the formula $\Delta G^\circ = -RT\cdot\ln K$. The experimental evidence shows that the abundance of the TSAP isomer is progressively

dx.doi.org/10.1021/ic201393n | Inorg. Chem. 2012, 51, 170−178

decreasing moving to the right across the lanthanide series.[8−11] Our calculations indeed predict a stabilization of the SAP isomer upon decreasing the ionic radius of the metal ion, in good agreement with the experimental results (Figure 1, see also Table 2). Furthermore, our calculations predict a slight

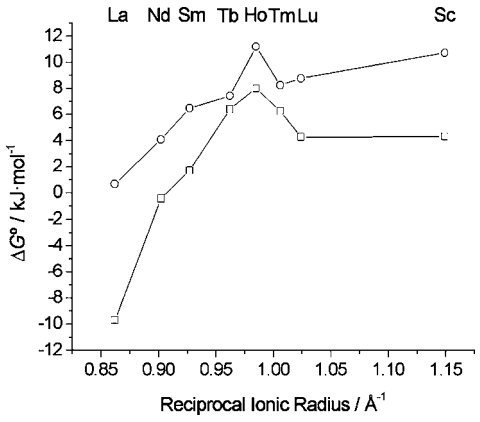

Figure 1. Experimental (□) and calculated (○) relative free energies for the SAP ⇆ TSAP equilibrium in $[Ln(DOTA)(H_2O)]^-$ (Ln = La−Ho), $[Ln(DOTA)]^-$ (Ln = Tm, Lu) and $[Sc(DOTA)]^-$ complexes versus the reciprocal ionic radius of the metal ion. Positive free energies indicate that the SAP isomer is more stable than the TSAP one.

Table 2. Relative Free Energies ($\Delta G°$) for the SAP ⇆ TSAP Equilibrium in $[Ln(DOTA)(H_2O)]^-$ (Ln = La, Nd, Sm), $[Ln(DOTA)]^-$ (Ln = Tm, Lu), and $[Sc(DOTA)]^-$ Complexes ($kJ·mol^{-1}$)[a]

Ln	La	Nd	Sm	Tm	Lu	Sc
$\Delta G°_{calcd}$	0.67	4.10	6.49	8.25	8.75	10.72
$\Delta G°_{exp}$	−9.71	−0.42	1.72	6.28	4.27	4.31

[a]Relative free energies are defined as $\Delta G° = G°_{TSAP} - G°_{SAP}$; note that the actual values of the complex free energies are negative, and therefore a positive relative free energy indicates that the SAP isomer is more stable than the TSAP one.

stabilization of the TSAP isomer for the heaviest lanthanides, in good agreement with the experimental trend. This stabilization of the TSAP form is most likely due to a change of the coordination number from 9 to 8 along the lanthanide series as a result of the expulsion of the inner sphere water molecule upon going to the smallest lanthanides (Tm−Lu). It must be pointed out that a hydration equilibrium is superimposed on the conformational equilibrium between SAP and TSAP isomers for the heaviest lanthanides (Tm−Lu), with both 8- and 9-coordinated species being observed for the TSAP forms.[11] However, only 8-coordinated species were considered in our calculations for the Tm^{3+} and Lu^{3+} complexes to avoid difficulties associated with the calculation of relative energies between species involved in a hydration equilibrium (i.e., standard state correction[35] and basis set superposition errors[36]). While being a relatively crude model, our calculations reproduce fairly well the experimental trend observed for the free energies between SAP and TSAP forms. Furthermore, the quantitative agreement between the experimental and calculated data is reasonably good, with differences between them of 10.5 $kJ·mol^{-1}$ for La and 0.8−6.3 $kJ·mol^{-1}$ for the Nd−Lu and Sc complexes (Table 2). Thus, we conclude that our computational approach reproduces fairly well the structures and energetics of Ln^{3+} and Sc^{3+} DOTA complexes.

Exchange between Bound and Unbound Oxygen Atoms of Acetate Groups. The exchange between the coordinated and non coordinated O-atoms of acetate groups was investigated for the $[Ln(DOTA)(H_2O)]^-$ (Ln = La, Nd, or Sm), $[Ln(DOTA)]^-$ (Ln = Tm or Lu), and $[Sc(DOTA)]^-$ systems. Additional calculations were also performed for the SAP isomers of $[Ln(DOTA)(H_2O)]^-$ complexes (Ln = Tm, Lu), for which the experimental evidence points to the presence of a coordinated water molecule.[11] However, in the latter cases attempts to model the carboxylate rotation process failed, geometry optimizations of the relevant transition states (TSs) leading to molecular geometries where an unbound carboxylate unit was involved in strong hydrogen-bonding interaction with the coordinated water molecule. For the remaining systems investigated exchange between bound and unbound oxygen atoms of acetate groups involves a rotation of the N−C−C−O dihedral angles of acetate groups, leading to a TS in which the distances between the O-atoms of the acetate involved in the rotation process and the lanthanide ion are considerably longer than in the reactant. Figure 2 shows the representative

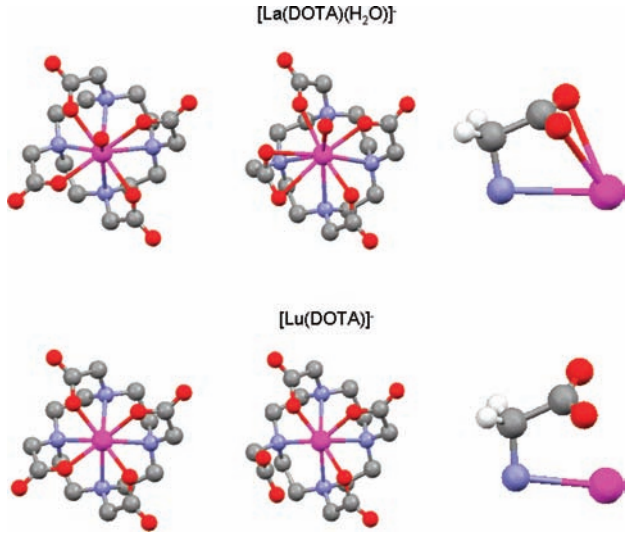

Figure 2. Structures of the energy minima for the SAP isomers of $[La(DOTA)(H_2O)]^-$ and $[Lu(DOTA)]^-$ complexes (left) and the TSs of the carboxylate rotation (center). The right column shows expansions around the rotating carboxylate of the TSs. In the TS, the Ln−O distances are 2.9 and 3.2 Å for La and Lu, respectively.

cases of energy minima and TSs for the SAP isomers of La^{3+} and Lu^{3+} complexes. According to our calculations, the rotation of the carboxylate group for the largest Ln^{3+} ions does not require a full decoordination of the pendant arm, which in the TS binds to the metal ion in a nearly symmetrical bidentate fashion. This situation is observed for both the SAP and the TSAP isomers, the distances between the Ln^{3+} ion and the O-atoms of the bidentate acetate group in the TS amounting to 2.73 and 2.86 Å for the TSAP isomer of the La^{3+} complex. The formation of the TS requires an important deformation of the metal coordination environment (Figure 2).

In TSs, the distances of the Ln^{3+} ion to O-atoms of the acetate group undergoing the rotation process gradually increase along the lanthanide series, reaching values of 3.23

dx.doi.org/10.1021/ic201393n | Inorg. Chem. 2012, 51, 170−178

and 3.26 Å (SAP), and 3.68 and 3.74 Å (TSAP) for the Lu^{3+} complexes. Thus, the interaction of the rotating carboxylate group and the Ln^{3+} ion in the TS is weakened as the ionic radius of the Ln^{3+} ions decreases, being in fact fully decoordinated in the case of the smallest lanthanides and Sc^{3+}. This results in smaller changes of the remaining bond distances of the metal coordination environment for the small lanthanides going from the ground to the TS.

The activation free energies for the carboxylate rotation process show a steady increase along the lanthanide series from La^{3+} to Lu^{3+} (Figure 3, see also Supporting Information, Table S2),

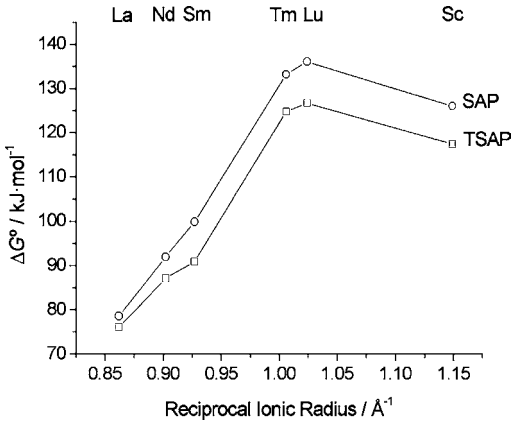

Figure 3. Activation free energies from DFT calculations performed in the gas-phase for the carboxylate rotation process in SAP (○) and TSAP (□) isomers of $[Ln(DOTA)(H_2O)]^-$ (Ln = La–Sm), $[Ln(DOTA)]^-$ (Ln = Tm, Lu), and $[Sc(DOTA)]^-$ complexes.

with values of ~75 kJ·mol^{-1} for La^{3+} and ~126 kJ·mol^{-1} for Lu^{3+}. This can be attributed to (i) the decrease in space for the coordination of the oxygen atoms of the rotating carboxylate in the TS, and (ii) the increasing charge density of the metal ion. A slight decrease of the activation free energies for the rotation of the carboxylate group is predicted upon decreasing the ionic radius of the metal ion from Lu^{3+} to Sc^{3+}. This effect can be explained by the stabilization of the 7-coordinate transition state in the Sc^{3+} analogue because of the smaller size of the metal ion. The activation energies calculated in the gas phase are slightly higher for the SAP isomers than for the TSAP forms.

Single point energy calculations in aqueous solution (PCM model) were performed at all critical points to evaluate the effects of the solvent in the energy barriers involved in the carboxylate rotation process. Our results show that the inclusion of solvent effects has a relatively small impact in the calculated free energy values, which decrease by ~8–21 kJ·mol^{-1} in solution with respect to the gas-phase (Supporting Information, Table S2). The lower energy barriers calculated in solution are probably the result of a more efficient solvation of the carboxylate group undergoing the rotation process in the transition state in comparison to the ground state. This effect is magnified on proceeding to the right across the series because of the complete decoordination of the acetate pendant in the TS. The free energy barriers for the carboxylate rotation process calculated for the SAP and TSAP isomers in aqueous solution are very similar, differing by less than 12.6 kJ·mol^{-1}.

Variable Temperature ^{17}O NMR Measurements. With the aim to verify the conclusions of the computations with experimental evidence, variable temperature ^{17}O NMR measurements were performed on Ln- and Sc-DOTA complexes with about 2% ^{17}O-enriched carboxylate functions. The ^{17}O-enriched ligand was obtained by heating the acid in 2% ^{17}O-enriched water at 363 K for 18 h, followed by lyophilization. All samples had a small excess of free ligand (≤5 mol %), which has a single resonance for the carboxylate groups at 278 ppm at pH 6.3 and 298 K and at 18.8 T.

Separate ^{17}O resonances were observed for Ln-DOTA and the free ligand, demonstrating that the exchange between complex and free ligand is slow on the NMR time scale, as should be expected. The spectra of the diamagnetic La-DOTA complex showed a single carboxylate ^{17}O resonance at 295–302 ppm between 25 and 147 °C, and at magnetic fields of 7.0, 9.4, and 18.8 T. Apparently, the exchange between the two carboxylate ^{17}O resonances is rapid on the NMR time scale under the conditions applied. The linewidths of these resonances decreased significantly upon increase of the temperature (see Supporting Information, Figure S1), which might be ascribed to the decrease of the rotational correlation time and the associated enhancement of the quadrupole relaxation time, which is the predominant ^{17}O NMR relaxation mechanism of diamagnetic compounds in the absence of exchange.[37] In addition there might be a decrease in line width because of a decrease of exchange broadening.

The ^{17}O NMR spectra of the paramagnetic Pr- and Sm-DOTA complexes and that of the diamagnetic Lu- and Sc-DOTA complexes each displayed two resonances of equal intensities (see Figure 4 and Supporting Information, Figure S1).

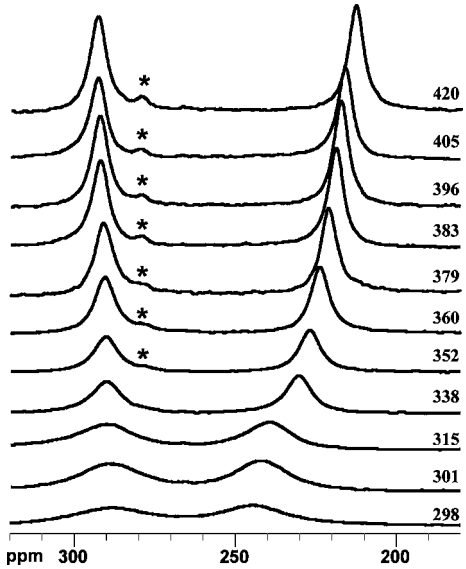

Figure 4. ^{17}O NMR spectra of $Sm(DOTA)^-$ at 18.8 T at different temperatures (K). The line width of the signal is clearly decreasing with the temperature. The resonance for the excess free ligand is indicated with an asterisk. For the spectra of the other compounds see Supporting Information, Figure S1.

One of the resonances of Lu-DOTA and the resonance of free DOTA are superimposed. The carboxylate ^{17}O resonances for $Sc(DOTA)^-$ almost coincided; an asymmetric signal was observed that could be deconvoluted into two Lorentzian peaks of equal intensity. No resonances could be observed for the DOTA complexes of heavier paramagnetic Ln^{3+} ions (Dy^{3+}, Ho^{3+}, and Yb^{3+}), probably because of excessive line broadening

dx.doi.org/10.1021/ic201393n | Inorg. Chem. 2012, 51, 170–178

as a result of their relatively large effective magnetic moment. The assignments of the ^{17}O resonances in the spectra for Pr- and Sm-DOTA were made on the basis of the temperature behavior of their chemical shifts. For one of the two signals for each of these complexes, the chemical shift was almost constant, whereas the other showed a relatively large temperature dependence (see Figure 5). The ^{17}O chemical shifts of these paramagnetic complexes consist of diamagnetic and paramagnetic contributions. The former shifts can be approximated by interpolation of the shifts of the diamagnetic La^{3+} and Lu^{3+} complexes. Hence, these shift contributions are about 270−300 ppm. The paramagnetic lanthanide induced shifts of Ln-bound O-atoms are known to be mainly of contact origin,[38] and this shift contribution is proportional to T^{-1}. The induced shifts of the unbound O-atoms are usually negligible with respect to those of bound ones, which explains the difference in magnitude of the temperature dependence of the chemical shifts of those oxygens. The sign and the magnitude of the contact shift contribution is dependent on the Ln^{3+} ion in question.[38] It is known that the contact shifts of isostructural Pr and Sm complexes have a ratio of −13.2, which is in agreement with the large difference in the chemical shifts observed for the Ln-bound O-atoms of the Pr- and Sm-DOTA complexes as well as with the opposite direction of the location of the resonances with respect to those of the corresponding diamagnetic La- and Lu-complexes. Since the diamagnetic shift contributions have a relatively small temperature dependence, the temperature dependence of the overall shifts are dominated by the temperature dependence of the contact shift and obviously, the overall chemical shifts of the Ln-bound O-atoms in Pr and Sm-DOTA move in opposite directions upon increase of the temperature.

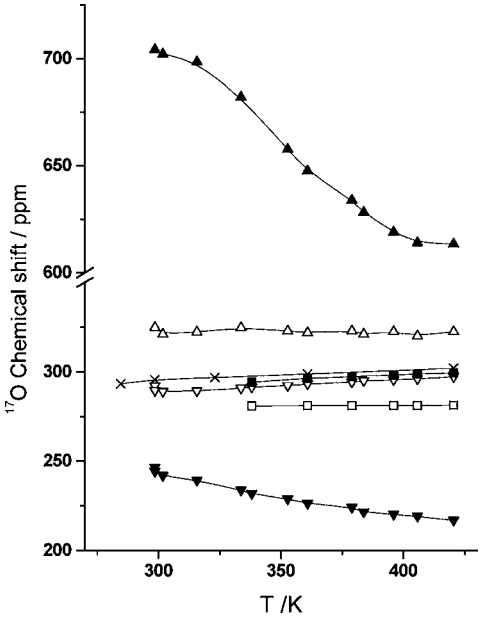

Figure 5. ^{17}O chemical shifts of the carboxylate oxygens in $Ln(DOTA)^-$ complexes as a function of temperature. (×) Ln = La (averaged signal for Ln-bound and unbound O); (up triangles), Ln = Pr; (down triangles) Ln = Sm; (squares) Ln = Lu. The chemical shifts for Ln-bound O-atoms are marked with filled symbols and those for Ln-unbound O-atoms with open symbols. The curves are guides of eyes.

Once again, the line width of these resonances decreases upon increase of the temperature (see Figure 4, Supporting Information, Figure S1d and Table S3). No coalescence of the two carboxylate ^{17}O resonances was observed for these complexes up to the highest temperatures investigated (420 K). Upon heating the samples, initially even a decrease of linewidths was observed (see also discussion of the transverse relaxation rates below). Only at the highest temperatures investigated, the resonances of Pr-DOTA (>390 K) and Sm-DOTA (>400 K) started to broaden again.

The ^{17}O NMR chemical shifts of the carboxylate resonances of various $Ln(DOTA)^-$ complexes are compiled in Table 3.

Table 3. ^{17}O NMR Chemical Shifts of Carboxylate Resonances of the Various $Ln(DOTA)^-$ Complexes at 298 K and 18.8 T

Ln	Ln−*O*−C=O	Ln−O−C=*O*
Sc	291.6	283.7
La	295.7[a]	
Pr	704.2	324.9
Sm	244.2	289.5
Lu	282.5	300.9

[a]Averaged resonance observed.

All these complexes occur as two diastereomeric forms in aqueous solution[11] and therefore theoretically two pairs of resonances should be found. This is clearly not observed, and the following explanations are possible: (i) the exchange between diastereometric forms is fast on the ^{17}O NMR time scale; (ii) the chemical shift difference between the SAP and the TSAP forms is small compared to the line width of the peaks; (iii) the amount of the minor form is much smaller than that of the major form. The latter explanation is unlikely, since it is known that the SAP and TSAP forms both occur in substantial amounts in aqueous samples of Pr- and Sm-DOTA.[8,9,11]

The observation of separate resonances for both oxygens in a carboxylate is rather uncommon. Generally, only a single averaged ^{17}O NMR signal is observed in aqueous samples of uncomplexed carboxylic acids and carboxylates at 250−260 ppm, because of intermolecular proton transfer and electron delocalization, respectively.[39] Separate signals may appear for carboxylic acids in dimethylsulfoxide (DMSO) solution at about 175 and 340 ppm, where the proton exchange rate is strongly reduced by hydrogen bonding effects.[39]

The transverse relaxation rates ($1/T_{2obs}$) of the various Ln-DOTA complexes were evaluated from the linewidths and are depicted as a function of the temperature in Figure 6 (see also Supporting Information, Table S3). The observed relaxation rates for slow and fast exchange between the carboxylate oxygen atoms on the NMR time scale can be approximated by eqs 1 and 2, respectively.[40−42]

$$\frac{1}{T_{2obs,A}} = \frac{1}{T_{2A}} + \frac{1}{\tau_M}; \quad \frac{1}{T_{2obs,B}} = \frac{1}{T_{2B}} + \frac{1}{\tau_M} \tag{1}$$

$$\frac{1}{T_{2,obs}} = \frac{0.5}{T_{2A}} + \frac{0.5}{T_{2B}} + 0.5\tau_M\Delta\omega_{AB}^2 \tag{2}$$

$$\frac{1}{T_{2,X}} = \frac{1}{T_{2,X}^{298}} \exp\left[\frac{E_A}{R}\left(\frac{1}{T} - \frac{1}{298.15}\right)\right]$$

$$X = A, B \tag{3}$$

dx.doi.org/10.1021/ic201393n | Inorg. Chem. 2012, 51, 170−178

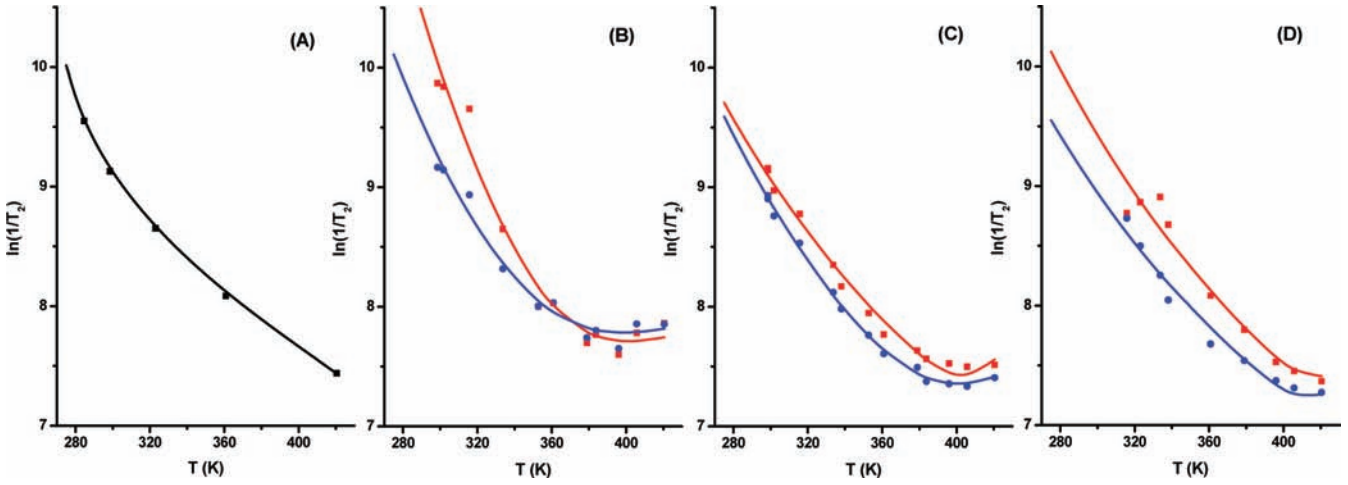

Figure 6. Transverse relaxation rates of the different Ln-DOTA complexes as function of the temperature at 18.8 T. Ln = La (A), Pr (B), Sm (C), Lu (D). The curves were calculated with the best-fit parameters (see Table 4) of fitting of the experimental data with eqs 2–4 (curve A) or eqs 1, 3, 4 (curves B-D), see text.

Table 4. Parameters Obtained from Least-Squares Fits ^{17}O NMR Transverse Relaxation Rates of Carboxylate Resonances of the Various Ln(DOTA)$^-$ Complexes at Variable Temperature and 18.8 T

Ln	τ_M^{298} (s)	$\Delta H^{\ddagger a}$ (kJ·mol^{-1})	$1/T_{2,A}^{298}$ (10^3 s^{-1})	E_A (kJ·mol^{-1})	$1/T_{2,B}^{298}$ (10^3 s^{-1})	E_B (kJ·mol^{-1})
La	$(1.7 \pm 0.1) \times 10^{-5}$	73.51	86 ± 0.8^b	13.9 ± 0.1^b	8.65 ± 0.08^b	13.8 ± 0.1^b
Pr	$(1.9 \pm 0.2) \times 10^{-3}$	84.8	23.0 ± 2.1	36.0 ± 2.7	10.2 ± 0.9	25.6 ± 2.6
Sm	$(1.2 \pm 0.2) \times 10^{+2}$	94.3	9.0 ± 0.3	17.6 ± 0.6	7.2 ± 0.2	17.0 ± 0.6
Lu	$(3.9 \pm 1.6) \times 10^{+4}$	135.8	12.9 ± 1.4	19.3 ± 1.6	8.0 ± 0.9	16.7 ± 1.6

[a]Fixed during fitting. Value obtained from DFT computations. The weighted average of the various conformers of the Ln under study was used. The value for Pr was estimated by interpolation of those computed for the other lanthanides. [b]Fast exchange, value for averaged signal.

$$\tau_M = \frac{298.15 \times \tau_M^{298}}{T} \exp\left[\frac{\Delta H^{\ddagger}}{R}\left(\frac{1}{T} - \frac{1}{298.15}\right)\right] \quad (4)$$

Here, A and B denote the free and the bound states of the carboxylate O-atoms, τ_M is the residence time of the nucleus in each of these states, $\Delta\omega_{AB}$ is the difference in their resonance frequencies in rad s^{-1}, $1/T_{2A}$ and $1/T_{2B}$ are their intrinsic transverse relaxation rates, $\Delta H^{\ddagger}$ is the enthalpy of activation, E_A and E_B are the activation energies associated with relaxation rates of A and B, and the symbols labeled with 298 represent values of parameters at 298.15 K. $1/T_{2A}$ and $1/T_{2B}$ are governed by the quadrupolar mechanism and are proportional to τ_R. The investigated complexes of paramagnetic lanthanides have dipolar and scalar contributions as well, which all are proportional to electronic relaxation rates, which are not very sensitive to temperature. Hence overall, $1/T_{2A}$ and $1/T_{2B}$ of these complexes decrease upon increase of the temperature.

The exchange of the carboxylate oxygens is slow for Lu- and Sc-DOTA and fast for La-DOTA under all conditions applied. If it is assumed that the chemical shift difference $\Delta\omega_{AB}$ is about the same for these compounds, it can be concluded that τ_M is larger for Lu and Sc than for La. For the complexes with slow exchange, the observed relaxation rates initially decrease upon increase of the temperature, because under those conditions the decrease of the relaxation rates $1/T_{2A}$ and $1/T_{2B}$ dominates. At higher temperatures, the effect of the decrease of τ_M gains in importance and then the observed relaxation rates start to increase again. The position of the minima in Figure 6 and the shape of the curves suggest that the τ_M values of these complexes increase in the order Pr-DOTA < Sm-DOTA < Lu-DOTA.

Attempts to fit the observed transverse relaxation rates with eqs 1 and 2 and single-exponential Eyring type equations to deal with the temperature dependences of the intrinsic relaxation rates and τ_M (see eqs 3 and 4) gave good fits, but unfortunately, the obtained best-fit parameters were meaningless because the parameters are strongly correlated and their standard deviations were larger than their values. However, if $\Delta H^{\ddagger}$ was fixed at the values obtained from the DFT calculations, excellent fits were obtained. The best-fit-values are compiled in Table 4, and Figure 6 displays the curves calculated with them. For Sc-DOTA the resonances could only be separated by deconvolution, which resulted in inaccurate linewidths and therefore, these data were not included into the fittings. The results obtained from the fittings must be taken with some care (i) since they are substantially affected by the $\Delta H^{\ddagger}$ values fixed during the fitting procedure, and (ii) the computed $\Delta H^{\ddagger}$ values were obtained with a relatively crude computational approach, and thus they might be not very accurate. However, the large differences in the value of τ_M^{298} among the lanthanides dramatically show the effect of the ionic radius on the rotation rate of the carboxylate function.

Effect of Addition of Co^{2+}. With the aim to change the NMR time scale of the carboxylate oxygen exchange of the diamagnetic Ln- and Sc-DOTA complexes by increasing $\Delta\omega_{AB}$, $CoCl_2$ was added stepwise to the samples. Because of the kinetic inertness of Ln- and Sc-DOTA complexes, transmetalation of the complexes with Co^{2+} will be negligible. Co^{2+} was selected because we expected that, because of its lower charge, it coordinates relatively weakly with carboxylate oxygens

dx.doi.org/10.1021/ic201393n | Inorg. Chem. 2012, 51, 170–178

of Ln- and Sc-DOTA. The first portion of $CoCl_2$ was complexed by the small excess of free ligand (≤5 mol %) present in the samples, as reflected by the disappearance of its resonance because of severe broadening. After that, the almost coinciding free carboxylate O-resonances of Lu- and Sc-DOTA showed an increasing chemical shift and line width with increase of the molar ratio Co^{2+}/M-DOTA (M = Lu, Sc; see Figure 7), whereas the chemical shift and line-width of the

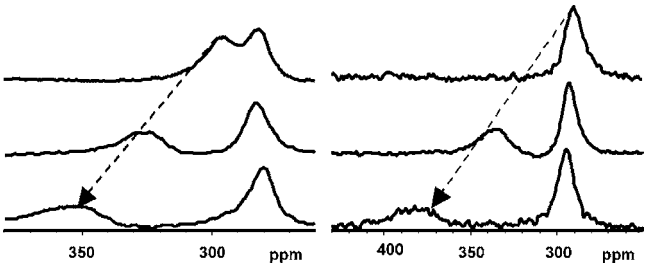

Figure 7. ^{17}O NMR spectra of Lu-DOTA (left) and Sc-DOTA (right) at 7 T and 368 K taken after the addition of 0, 10, and 15 mol % of $CoCl_2$ (top to bottom, respectively). The signal with the largest Co^{2+} induced shift and line broadening is assigned to the carboxylate oxygen that is not bound to Lu^{3+} or Sc^{3+}.

bound oxygen atoms were almost unaffected. These findings indicate that the exchange between the adduct of Co^{2+} and M-DOTA and free M-DOTA (M = Lu, Sc) is rapid on the ^{17}O NMR time scale. For La-DOTA, however, a shift and broadening of the averaged carboxylate ^{17}O signal was observed, whereas the exchange between the La-bound and unbound carboxylate oxygen atoms remained fast on the ^{17}O NMR time scale upon addition of Co^{2+}. The difference in behavior between La- and Lu- or Sc-DOTA in these experiments suggests that the exchange between the two oxygen atoms in each carboxylate group is much faster for La than for Lu and Sc, which again is in agreement with the results of the DFT calculations and the τ_M^{298} values reported in Table 4.

CONCLUSIONS

DFT computations predict that the mechanism and the rate of rotation of carboxylate oxygens in complexes of DOTA with Ln^{3+} and Sc^{3+} ions are strongly dependent on the radius of the central metal ion. For the larger metal ions, the rotation takes place via a transition state in which the carboxylate function is bound to the metal ion in a nearly symmetrical bidentate fashion with Ln−O distances that are somewhat elongated compared to the reactant. In the complexes of the smaller metal ions (Lu^{3+}, Sc^{3+}), such a transition state would be sterically very crowded and then a pathway via decoordination of the carboxylate oxygen is preferred. The activation free energies computed for the rotation process increase along the lanthanide series from about 75 to 125 and 135 kJ·mol^{-1} for the SAP and TSAP isomers, respectively. Although the accuracy of these values remains uncertain, and should be probably tested against high level ab initio calculations, our results are consistent with the results of a variable temperature ^{17}O NMR study on these systems. Thanks to the relatively slow rotation of the carboxylate group and the increased shift dispersion in paramagnetic systems, separate resonances were observed for the Ln^{3+}-bound and free carboxylate oxygen nuclei, except in La-DOTA, where the exchange of these oxygen atoms was rapid on the NMR time scale.

The activation free energies for the presently studied carboxylate rotation process are considerably higher than that for the exchange between Ln-bound water and bulk water for $[Ln(DOTA)(H_2O)]^-$ complexes and for the SAP/TSAP rearrangement. For example for $[Eu(DOTA)(H_2O)]^-$, $\Delta G^{\ddagger}_{306}$ has been determined to be about 35 kJ·mol^{-1} for the water exchange and 63 kJ·mol^{-1} for the conformational rearrangement.[11,43] Consequently, the corresponding rates are much faster than the rate of rotation of the carboxylate groups, and it is very likely that these processes are taking place independently of each other.

ASSOCIATED CONTENT

Supporting Information

Computed free energies of transition states involved in the carboxylate rotation process, optimized Cartesian Coordinates (Å) of energy minima and transition states, and ^{17}O NMR spectra and linewidths of the observed signals. This material is available free of charge via the Internet at http://pubs.acs.org.

AUTHOR INFORMATION

Corresponding Author

*E-mail: K.Djanashvili@tudelft.nl.

ACKNOWLEDGMENTS

Thanks are due to Prof. C. S. Springer, Jr. (Oregon Health and Science University, Portland, Oregon, U.S.A.) for helpful discussions, and to the Centro de Supercomputación de Galicia (CESGA) for providing the computer facilities. This work was done in the framework of COST Action D38 "Metal-Based Systems for Molecular Imaging Applications" and of the 3Binding project "Imaging, Interpretation and Therapy; Innovation in Nuclear Diagnostic and Therapy in Health Care", which is financially supported by the Dutch Ministry of Economic Affairs and by the Province of Zuid-Holland.

REFERENCES

(1) Desreux, J. F. *Inorg. Chem.* **1980**, *19*, 1319−1324.
(2) Wang, X.; Jin, T.; Comblin, V.; Lopez-Mut, A.; Merciny, E.; Desreux, J. F. *Inorg. Chem.* **1992**, *31*, 1095−1099.
(3) Merbach, A. E.; Tóth, É. *The chemistry of contrast agents in medical magnetic resonance imaging*; John Wiley & Sons, Ltd: Chichester, U.K., 2001.
(4) Caravan, P.; Ellison, J. J.; McMurry, T. J.; Lauffer, R. B. *Chem. Rev.* **1999**, *99*, 2293−2352.
(5) Terreno, E.; Delli Castelli, D.; Viale, A.; Aime, S. *Chem. Rev.* **2010**, *110*, 3019−3042.
(6) Caravan, P. *Chem. Soc. Rev.* **2006**, *35*, 512−523.
(7) Aime, S.; Delli Castelli, D.; Geninatti Crich, S.; Gianolio, E.; Terreno, E. *Acc. Chem. Res.* **2009**, *42*, 822−831.
(8) Aime, S.; Botta, M.; Ermondi, G. *Inorg. Chem.* **1992**, *31*, 4291−4299.
(9) Hoeft, S.; Roth, K. *Chem. Ber.* **1993**, *126*, 869−873.
(10) Jacques, V.; Desreux, J. F. *Inorg. Chem.* **1994**, *33*, 4048−4053.
(11) Aime, S.; Botta, M.; Fasano, M.; Marques, M. P. M.; Geraldes, C. F. G. C.; Pubanz, D.; Merbach, A. E. *Inorg. Chem.* **1997**, *36*, 2059−2068.
(12) Aime, S.; Barge, A.; Botta, M.; De Sousa, A. S.; Parker, D. *Angew. Chem., Int. Ed.* **1998**, *37*, 2673−2675.
(13) Dunand, F. A.; Aime, S.; Merbach, A. E. *J. Am. Chem. Soc.* **2000**, *122*, 1506−1512.
(14) Woods, M.; Aime, S.; Botta, M.; Howard, J. A. K.; Moloney, J. M.; Navet, M.; Parker, D.; Port, M.; Rousseaux, O. *J. Am. Chem. Soc.* **2000**, *122*, 9781−9792.

(15) Dunand, F. A.; Dickins, R. S.; Parker, D.; Merbach, A. E. *Chem.—Eur. J.* **2001**, *7*, 5160−5167.
(16) Zhang, S.; Kovacs, Z.; Burgess, S.; Aime, S.; Terreno, E.; Sherry, A. D. *Chem.—Eur. J.* **2001**, *7*, 288−296.
(17) Powell, D. H.; NiDhubhghaill, O. M.; Pubanz, D.; Helm, L.; Lebedev, Y. S.; Schlaepfer, W.; Merbach, A. E. *J. Am. Chem. Soc.* **1996**, *118*, 9333−9346.
(18) Purgel, M.; Baranyai, Z.; de Blas, A.; Rodríguez-Blas, T.; Bányai, I.; Platas-Iglesias, C.; Tóth, I. *Inorg. Chem.* **2010**, *49*, 4370−4382.
(19) Cusanelli, A.; Frey, U.; Richens, D. T.; Merbach, A. E. *J. Am. Chem. Soc.* **1996**, *118*, 5265−5271.
(20) Helm, L. *NMRICMA*, 3.1.5; EPFL: Lausanne, Switzerland, 2003.
(21) Becke, A. D. *J. Chem. Phys.* **1993**, *98*, 5648−5652.
(22) Lee, C.; Yang, W.; Parr, R. G. *Phys. Rev. B* **1988**, *37*, 785−789.
(23) Frisch, M. J.; Trucks, G. W.; Schlegel, H. B.; Scuseria, G. E.; Robb, M. A.; Cheeseman, J. R.; Scalmani, G.; Barone, V.; Mennucci, B.; Petersson, G. A.; Nakatsuji, H.; Caricato, M.; Li, X.; Hratchian, H. P.; Izmaylov, A. F.; Bloino, J.; Zheng, G.; Sonnenberg, J. L.; Hada, M.; Ehara, M.; Toyota, K.; Fukuda, R.; Hasegawa, J.; Ishida, M.; Nakajima, T.; Honda, Y.; Kitao, O.; Nakai, H.; Vreven, T.; Montgomery, Jr., J. A.; Peralta, J. E.; Ogliaro, F.; Bearpark, M.; Heyd, J. J.; Brothers, E.; Kudin, K. N.; Staroverov, V. N.; Kobayashi, R.; Normand, J.; Raghavachari, K.; Rendell, A.; Burant, J. C.; Iyengar, S. S.; Tomasi, J.; Cossi, M.; Rega, N.; Millam, N. J.; Klene, M.; Knox, J. E.; Cross, J. B.; Bakken, V.; Adamo, C.; Jaramillo, J.; Gomperts, R.; Stratmann, R. E.; Yazyev, O.; Austin, A. J.; Cammi, R.; Pomelli, C.; Ochterski, J. W.; Martin, R. L.; Morokuma, K.; Zakrzewski, V. G.; Voth, G. A.; Salvador, P.; Dannenberg, J. J.; Dapprich, S.; Daniels, A. D.; Farkas, Ö.; Foresman, J. B.; Ortiz, J. V.; Cioslowski, J.; Fox, D. J. *Gaussian 09*, Revision A.02; Gaussian, Inc.: Wallingford, CT, 2009.
(24) Regueiro-Figueroa, M.; Esteban-Gómez, D.; de Blas, A.; Rodríguez-Blas, T.; Platas-Iglesias, C. *Eur. J. Inorg. Chem.* **2010**, 3586−3595.
(25) Dolg, M.; Stoll, H.; Savin, A.; Preuss, H. *Theor. Chim. Acta* **1989**, *75*, 173−194.
(26) Maron, L.; Eisenstein, O. *J. Phys. Chem. A* **2000**, *104*, 7140−7143.
(27) Eisenstein, O.; Maron, L. *J. Organomet. Chem.* **2002**, *647*, 190−197.
(28) (a) Peng, C.; Ayala, P. Y.; Schlegel, H. B.; Frisch, M. J. *J. Comput. Chem.* **1996**, *17*, 49−56. (b) Peng, C.; Schlegel, H. B. *Isr. J. Chem.* **1994**, *33*, 449−454.
(29) Tomasi, J.; Mennucci, B.; Cammi, R. *Chem. Rev.* **2005**, *105*, 2999−3093.
(30) Benetollo, F.; Bombieri, G.; Calabi, L.; Aime, S.; Botta, M. *Inorg. Chem.* **2003**, *42*, 148−157.
(31) Seitz, M.; Oliver, A. G.; Raymond, K. N. *J. Am. Chem. Soc.* **2007**, *129*, 11153−11160.
(32) (a) Heiberg, H.; Gropen, O.; Laerdahl, J. K.; Swang, O.; Wahlgren, U. *Theor. Chem. Acc.* **2003**, *110*, 118−125. (b) Buzko, V.; Sukhno, I.; Buzko, M. *THEOCHEM* **2009**, *894*, 75−79.
(33) Cosentino, U.; Moro, G.; Pitea, D.; Barone, V.; Villa, A.; Muller, R. N.; Botteman, F. *Theor. Chem. Acc.* **2004**, *111*, 204−209.
(34) (a) Tsushima, S.; Yang, T.; Mochizuki, Y.; Okamoto, Y. *Chem. Phys. Lett.* **2003**, *375*, 204−212. (b) Li, H.; Jensen, J. H. *J. Comput. Chem.* **2004**, *25*, 1449−1462.
(35) Bryantsev, V. S.; Diallo, M. S.; Goddard, W. A. III *J. Phys. Chem. B* **2008**, *112*, 9709−9719.
(36) (a) Dunescu, A.; Clark, A. E. *J. Phys. Chem. A* **2008**, *112*, 11198−11206. (b) Kvamme, B.; Wander, M. C. F.; Clark, A. E. *Int. J. Quantum Chem.* **2009**, *109*, 2474−2481.
(37) Gerothanassis, I. P. *Prog. Nucl. Magn. Reson. Spectrosc.* **2010**, *56*, 95−197.
(38) Peters, J. A.; Huskens, J.; Raber, D. J. *Progr. Nucl. Magn.Reson. Spectrosc.* **1996**, *28*, 283−350.
(39) Theodorou, V.; Troganis, A. N.; Gerothanassis, I. P. *Tetrahedron Lett.* **2004**, *45*, 2243−2245.
(40) Swift, T. J.; Connick, R. E. *J. Chem. Phys.* **1962**, *37*, 307−320.
(41) Leigh, J. S. Jr. *J. Magn. Reson.* **1971**, *4*, 308−311.
(42) McLaughlin, A. C.; Leigh, J. S. Jr. *J. Magn. Reson.* **1973**, *9*, 296−304.
(43) Micskei, K.; Helm, L.; Brücher, E.; Merbach, A. E. *Inorg. Chem.* **1993**, *32*, 3844−3850.